Tsuneo Yoshikawa
Xin-Zhi Zheng
Department of Mechanical Engineering
Kyoto University
Kyoto 606, Japan

Coordinated Dynamic Hybrid Position/Force Control for Multiple Robot Manipulators Handling One Constrained Object

Abstract

In coordinated manipulation of a single object using multiple robot arms or a multifingered robot hand, simultaneous control of the object motion and of the internal force exerted by arms or fingers on the object is required. Furthermore, in the case where the motion of the object is constrained in some directions because of contact with its environment, control of the constraint force also becomes necessary. In this article, we propose a coordinated dynamic hybrid control method for multiple robotic mechanisms. The method takes the manipulator dynamics and object dynamics into consideration and controls the motion of an object under constraint as well as the constraint force and the internal force. The motion control of an object in free space can be treated as a special case within the same formulation. A unified description for accommodating various grasp types is used. Several experimental results that show the validity of the proposed approach are presented. The results of this article will be useful for fine manipulation tasks using multiple robotic mechanisms, where the individual specifications of the object motion, the interaction force between the object and its environment, and the grasping force of the object are given.

1. Introduction

There is growing interest in the development of coordinated multiple manipulator systems, since in a variety of tasks using a robot manipulator, it is often necessary to use two or more robot arms rather than one to perform a task. For instance, a manipulated object may be too heavy to be handled by a single arm. On the other hand, multifingered robot hands are indispensable for skillful grasping and dexterous manipulation of objects.

The International Journal of Robotics Research,
Vol. 12, No. 3, June 1993.

On those occasions when multiple robotic mechanisms grasp and manipulate a common object cooperatively, usually it is necessary to control the motion of the manipulated object; at the same time, the internal force, which is exerted on the object by the arms or fingers but does not affect the object motion, must be decided and controlled appropriately as a result of the redundancy of the end-effector force. A number of researchers have tackled this force distribution problem and the coordinated control problem. Nakano et al. (1974) and Arimoto et al. (1987) applied a master-slave approach to the two-arm robot problem. Luh and Zheng (1987) studied the kinematic relations between two coordinated robots in handling several different objects. Zheng and Luh (1989) and Alberts and Soloway (1988) used the criterion of minimum energy consumption of joint torques or of exerted forces in task space, in terms of their least square norm, to solve the redundancy problem when determining the joint driving force. The internal force, however, is not controlled directly in the latter three studies, although it is kept small. In a different approach, Uchiyama and Dauchez (1988) proposed a symmetric hybrid position/internal force control scheme for the coordination of two robots. Yoshikawa and Nagai (1987), Kumar and Waldron (1988), and Nakamura et al. (1989) proposed methods to determine the internal force. Li et al. (1989) proposed a task-oriented grasp planning and dynamic coordinated control algorithm for a multifingered robot hand.

Including the above research efforts, most research on coordinated control of two or more robotic mechanisms so far has concentrated on the problem in free space. However, in further applications of the multiple robotic mechanisms to such tasks as bolt assembly or line drawing, the motion of the held object is constrained in some directions because of interaction between the object and the environment. In such tasks, it is often nec-

essary to control the constraint force interacting between them in addition to the motion of the object. For a single manipulator, Raibert and Craig (1981) formulated the hybrid position/force control scheme, and Yoshikawa (1987) proposed the dynamic hybrid control method, which describes the constraints on the end effector by a set of hypersurfaces and takes arm dynamics into account. Those schemes, however, cannot be applied directly to the multiple robot problem in their original forms. Hayati (1986) employed an extension of Raibert and Craig's (1981) hybrid control for a multiarmed robot by partitioning the object and regarding the object segments as part of the last link of each arm, but without treating the internal force control explicitly. Khatib (1987) extended his operational space formulation for single manipulator motion and force control to a multieffector/object system with the end effectors grasping the object rigidly, though treating the system using an augmented object model. The results in the models in the latter two studies are not suitable for application to nonrigid grasping such as used with a multifingered hand.

In this article we propose a coordinated dynamic hybrid position/force control method for a set of robot arms or a multifingered robot hand handling a single object whose motion is constrained by its environment. This method takes the manipulator dynamics and object dynamics into consideration. First, we will give some basic formulations for coordinated control of a constrained object, including kinematics and dynamics of manipulators, object dynamics, force and kinematic constraint relations between manipulators and object, and hypersurface description of object motion constraint (Yoshikawa 1987), on which the dynamics of the whole system is derived. Then we will derive a nonlinear state feedback law that linearizes and decouples the system with respect to the object motion, the constraint force, and the internal force. We will present a structure of the control system consisting of this linearizing feedback law and a servo compensator. Note that the controlling of object motion in free space will be treated as a special case of the constrained object motion control formulated in this article. Finally, we will give several experimental results to show the validity of the proposed approach. Note that a unified description is used to apply this method to a set of coordinated multiple arms, a multifingered hand, or a combined arm-finger mechanism.

2. Basic Formulations for Coordinated Manipulation of a Constrained Object

Basic formulations for the coordinated control of an object that is constrained during its motion from the environment in some directions will be given in this section. The subjects in Sections 2.1 and 2.2 will be covered only briefly, as they are already discussed elsewhere in the literature (Li et al. 1989; Nakamura et al. 1989).

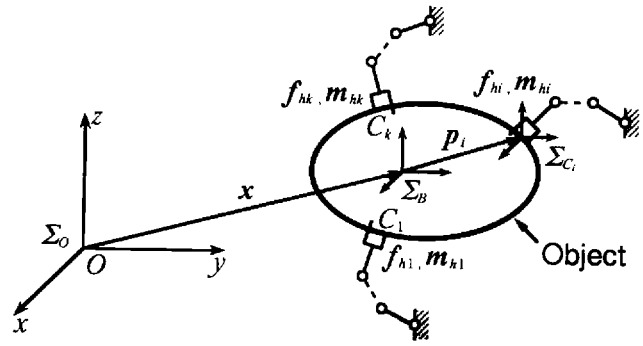

Fig. 1. Model of coordinated control.

Coordinated manipulation with k robot arms is shown in Figure 1. The interaction between each arm and the object will not be restricted to a specific type: it can include complete fixing by a gripper, frictional point contact, or frictionless point contact. We only assume that the contact point does not slip on the object in the case of point contact grasping. Consideration of the manipulation of objects using a multifingered robot hand where the interaction between the object and the fingers is a rolling contact will be also an important issue. However, this will result in a nonholonomic constraint problem with quite a different formulation and will not be considered in this article. The work by Cole et al. (1989) may provide some insight on the subject. A sliding case will also not be discussed here.

An object coordinate frame Σ_B is fixed at the mass center of the object, and the position and orientation of the object are denoted by, respectively, $\mathbf{x} \in \mathbf{R}^3$, the position vector of the origin of Σ_B, and $\mathbf{R}_B \in \mathbf{R}^{3\times 3}$. Here, the columns of $\mathbf{R}_B$ are unit vectors in the directions of the x, y, and z axes of Σ_B expressed in terms of the reference coordinate frame Σ_O. A set of grasp point frames $\Sigma_{C_i}(i = 1, 2, \cdots, k)$ are fixed at each arm's grasp point C_i on the object. The resultant force and torque applied on the object and the force and torque applied on C_i are defined with respect to the origin of Σ_B and the origin of Σ_{C_i}, respectively. Vectors are expressed in terms of Σ_O unless otherwise stated.

2.1. Kinematics and Dynamics of Manipulators

Let the position of the end effector of ith arm be denoted by $\mathbf{x}_{h_i} \in \mathbf{R}^3$; the velocity, including orientational elements, by $\mathbf{v}_{h_i} \triangleq [\dot{\mathbf{x}}_{h_i}^T \ \omega_{h_i}^T]^T \in \mathbf{R}^6$; and the joint variable vector by $\mathbf{q}_i \in \mathbf{R}^{n_i}$ $(n_i \geq 6)$. Letting $n = \sum_{i=1}^{k} n_i$, the kinematic equation for k arms can be written together as

$$\mathbf{v}_h = \mathbf{J}(\mathbf{q})\dot{\mathbf{q}}, \tag{1}$$

$$\dot{\mathbf{v}}_h = \mathbf{J}(\mathbf{q})\ddot{\mathbf{q}} + \dot{\mathbf{J}}(\mathbf{q})\dot{\mathbf{q}}, \tag{2}$$

and the dynamic equation is assumed to be given as

$$\mathbf{M}(\mathbf{q})\ddot{\mathbf{q}} + \mathbf{h}(\mathbf{q}, \dot{\mathbf{q}}) = \tau, \tag{3}$$

where

$$\mathbf{v}_h \triangleq [\mathbf{v}_{h_1}^T \cdots \mathbf{v}_{h_k}^T]^T \in \mathbf{R}^{6k},$$
$$\mathbf{J}(\mathbf{q}) \triangleq \mathrm{diag}[\mathbf{J}_1(\mathbf{q}_1), \cdots, \mathbf{J}_k(\mathbf{q}_k)] \in \mathbf{R}^{6k \times n},$$
$$\mathbf{q} \triangleq [\mathbf{q}_1^T \cdots \mathbf{q}_k^T]^T \in \mathbf{R}^n,$$
$$\mathbf{M}(\mathbf{q}) \triangleq \mathrm{diag}[\mathbf{M}_1(\mathbf{q}_1), \cdots, \mathbf{M}_k(\mathbf{q}_k)] \in \mathbf{R}^{n \times n},$$
$$\mathbf{h}(\mathbf{q}, \dot{\mathbf{q}}) \triangleq [\mathbf{h}_1^T(\mathbf{q}_1, \dot{\mathbf{q}}_1), \cdots, \mathbf{h}_k^T(\mathbf{q}_k, \dot{\mathbf{q}}_k)]^T \in \mathbf{R}^n,$$
$$\tau \triangleq [\tau_1^T \cdots \tau_k^T]^T \in \mathbf{R}^n.$$

Here, $\mathbf{J}_i(\mathbf{q}_i) \in \mathbf{R}^{6 \times n_i}$ is the Jacobian of the ith arm; $\mathbf{M}_i(\mathbf{q}_i) \in \mathbf{R}^{n_i \times n_i}$ is the inertia matrix; $\mathbf{h}_i(\mathbf{q}_i, \dot{\mathbf{q}}_i) \in \mathbf{R}^{n_i}$ represents the centrifugal, Coriolis, viscous, and gravitational forces; and $\tau_i \in \mathbf{R}^{n_i}$ is the joint driving force.

$\mathbf{J}(\mathbf{q})$, $\mathbf{M}(\mathbf{q})$, and $\mathbf{h}(\mathbf{q},\dot{\mathbf{q}})$ will be written as $\mathbf{J}$, $\mathbf{M}$, and $\mathbf{h}$ hereafter.

2.2. *Object Dynamics*

Let the mass of the object be m and its inertia tensor be $\mathbf{I} \in \mathbf{R}^{3\times3}$. Then the equation of motion of the object is given by $\mathbf{I}_B\dot{\mathbf{v}} + \mathbf{Q}_B = \mathbf{F}$ when the object velocity is denoted by $\mathbf{v} \triangleq [\dot{\mathbf{x}}^T \ \boldsymbol{\omega}^T]^T \in \mathbf{R}^6$, where $\mathbf{I}_B \triangleq \mathrm{diag}[m\mathbf{I}_3, \mathbf{I}] \in \mathbf{R}^{6\times6}$, $\mathbf{Q}_B \triangleq [-m\mathbf{g}^T \ \{\boldsymbol{\omega} \times (\mathbf{I}\boldsymbol{\omega})\}^T]^T \in \mathbf{R}^6$, $\mathbf{I}_n$ denotes an $n \times n$ unit matrix, and $\mathbf{g}$ denotes the acceleration resulting from gravity. $\mathbf{F} \triangleq [\mathbf{f}^T \ \mathbf{m}^T]^T \in \mathbf{R}^6$ is the force applied on the object.

Suppose the object velocity is given by the time derivative of a six-dimensional position vector $\mathbf{r} \triangleq [\mathbf{x}^T \ \phi^T]^T \in \mathbf{R}^6$, and the relation between $\mathbf{v}$ and $\dot{\mathbf{r}}$ is given by

$$\mathbf{v} = \mathbf{T}\dot{\mathbf{r}} \tag{4}$$

for an appropriate matrix $\mathbf{T} = \mathbf{T}(\mathbf{r}) \in \mathbf{R}^{6\times6}$. Using $\mathbf{r}$, the equation of motion of the object can be written as

$$\mathbf{I}_B\mathbf{T}\ddot{\mathbf{r}} + \mathbf{Q}_r = \mathbf{F}, \tag{5}$$

where $\mathbf{Q}_r \triangleq \mathbf{I}_B\dot{\mathbf{T}}\dot{\mathbf{r}} + [-m\mathbf{g}^T \ \{\boldsymbol{\omega} \times (\mathbf{I}\boldsymbol{\omega})\}^T]^T \in \mathbf{R}^6$. The orientational elements of $\mathbf{r}$, ϕ, can be given by Euler angles, or roll-pitch-yaw angles. When, for example, Euler angles (ϕ, θ, ψ) are used for ϕ, $\mathbf{T}$ is given by

$$\mathbf{T} = \mathrm{diag}[\mathbf{I}_3, \mathbf{T}_r], \tag{6}$$

$$\mathbf{T}_r \triangleq \begin{bmatrix} 0 & -S_\phi & C_\phi S_\theta \\ 0 & C_\phi & S_\phi S_\theta \\ 1 & 0 & C_\theta \end{bmatrix}, \tag{7}$$

where $S_\phi \triangleq \sin\phi$, $C_\phi \triangleq \cos\phi$, etc.

2.3. *Force and Kinematic Constraint Relations Between Arms and Object*

Depending on the grasping type, as noted earlier, the force and kinematic constraint relations between the end effector and the object will become different. Let

$$^C\mathbf{S}_i \triangleq [\mathbf{s}_{i1} \ \mathbf{s}_{i2} \ \cdots \ \mathbf{s}_{id_i}] \in \mathbf{R}^{6\times d_i} \tag{8}$$

express the constraint. In (8), $\mathbf{s}_{ij} \in \mathbf{R}^6 (j = 1, 2, \cdots, d_i, d_i \leq 6)$ are unit vectors expressed in Σ_{C_i} that denote the directions of independently applicable forces of the ith arm to the object and, at the same time, the directions in which no relative motion occurs between them. For instance, we may have $^C\mathbf{S}_i = \mathbf{I}_6$ for a grasp with a gripper by the ith arm, which can apply three translational forces and three moments to the object independently, with no relative motion between the gripper and the object; we also have $^C\mathbf{S}_i = [\mathbf{I}_3 \ \mathbf{O}_3]^T$ for holding by the ith arm (or finger) with frictional point contact, in which only three translational forces are applied and only the translational relative position is constrained. Also, this description of constraint relation can be developed for other types of end effectors without the applicable forces being restricted to be mutually orthogonal.

Then the constraint matrix expressed in Σ_O for the set of k arms is described by

$$\mathbf{S} = \mathrm{diag}[\mathbf{S}_1, \mathbf{S}_2, \cdots, \mathbf{S}_k] \in \mathbf{R}^{6k\times d}, \quad d = \sum_{i=1}^{k} d_i, \tag{9}$$

where $\mathbf{S}_i \triangleq \mathrm{diag}[\mathbf{R}_{C_i}, \mathbf{R}_{C_i}]\ ^C\mathbf{S}_i \in \mathbf{R}^{6\times d_i}$, and $\mathbf{R}_{C_i} \in \mathbf{R}^{3\times3}$ denotes the orientation of Σ_{C_i} with respect to Σ_O. Note that d satisfies $d \leq 6k$.

Introducing this description makes it possible to derive (1) a unified formulation for the force and kinematic constraint relation for holding an object with various types of end effector in a multiple manipulator system, and (2) the dynamic equation of such a system, derived later.

The same description can also be seen in, for example, Cutkosky and Kao (1989), where it played a fundamental role in transforming the fingertip stiffness matrix to the object coordinate frame. In this way a general expression for the effective grasp stiffness was developed, and the problem of controlling the desired overall grasp stiffness in quasistatic conditions through adjusting the finger joint servo gains was discussed.

2.3.1. *Force Relation*

Let $\mathbf{F}_{h_i} \triangleq [\mathbf{f}_{h_i}^T \ \mathbf{m}_{h_i}^T]^T \in \mathbf{R}^6$ denote the force exerted on the object by the ith arm. Under the constraint of (9), the actual force $\mathbf{F}_h \triangleq [\mathbf{F}_{h_1}^T \cdots \mathbf{F}_{h_k}^T]^T \in \mathbf{R}^{6k}$ exerted on the

object by the arms can be represented by

$$\mathbf{F}_h = \mathbf{S}\mathbf{F}_{hS}, \tag{10}$$

where $\mathbf{F}_{hS} \in \mathbf{R}^d$ is a vector representing the magnitudes of force components in the directions expressed by column vectors of $\mathbf{S}$. Then the resultant force applied on the object, $\mathbf{F} \triangleq [\mathbf{f}^T \ \mathbf{m}^T]^T \in \mathbf{R}^6$, is given by

$$\begin{aligned}\mathbf{F} &= \mathbf{W}\mathbf{F}_h \\ &= \mathbf{W}_S\mathbf{F}_{hS},\end{aligned} \tag{11}$$

where $\mathbf{W}_S \triangleq \mathbf{W}\mathbf{S} \in \mathbf{R}^{6\times d}$,

$$\mathbf{W} \triangleq \begin{bmatrix} \mathbf{I}_3 & \mathbf{0} & \mathbf{I}_3 & \mathbf{0} & \cdots & \mathbf{I}_3 & \mathbf{0} \\ \mathbf{P}_1 & \mathbf{I}_3 & \mathbf{P}_2 & \mathbf{I}_3 & \cdots & \mathbf{P}_k & \mathbf{I}_3 \end{bmatrix} \in \mathbf{R}^{6\times 6k},$$

and $\mathbf{P}_i \in \mathbf{R}^3$ is a skew-symmetric matrix expressing the cross-product from the position vector of Σ_{C_i} with respect to Σ_B.

It can be seen from (11) that matrix $\mathbf{W}_S$ must be of full rank to be able to manipulate an object freely in three-dimensional space, because arbitrary resultant forces $\mathbf{F} \in \mathbf{R}^6$ should be generated to achieve arbitrarily given object acceleration.[1]

Given the resultant force $\mathbf{F}$, the $\mathbf{F}_{hS}$ that satisfies (11) can be represented as

$$\mathbf{F}_{hS} = \mathbf{W}_S^+\mathbf{F} + \mathbf{A}_S\mathbf{f}_{IS}, \tag{12}$$

where $\mathbf{A}_S \in \mathbf{R}^{d\times(d-\mathrm{rank}\mathbf{W}_S)}$ is the matrix of orthonormals generated from the linearly independent vectors of the null space of $\mathbf{W}_S$ and $\mathbf{f}_{IS} \in \mathbf{R}^{d-\mathrm{rank}\mathbf{W}_S}$ is an arbitrary constant vector. Here $\mathbf{W}_S^+\mathbf{F}$ is the part of $\mathbf{F}_{hS}$ that generates $\mathbf{F}$, and $\mathbf{A}_S\mathbf{f}_{IS}$ represents the internal force element of $\mathbf{F}_{hS}$ that does not affect the resultant force $\mathbf{F}$.

2.3.2. *Kinematic Relation*

Let $\boldsymbol{\omega}_{C_i}$ denote the orientational velocity of Σ_{C_i}, and let $\mathbf{v}_{C_i} \triangleq [\dot{\mathbf{x}}_{C_i}^T \ \boldsymbol{\omega}_{C_i}^T]^T \in \mathbf{R}^6$. Then, from the duality and (4), we have

$$\mathbf{v}_C = \mathbf{W}^T\mathbf{T}\dot{\mathbf{r}}. \tag{13}$$

Assuming that the object and the end effectors of the arms do not slip at the contact points in the directions expressed by (9), the velocity vectors $\mathbf{v}_h$ and $\mathbf{v}_C$ must satisfy

$$\mathbf{S}^T(\mathbf{v}_h - \mathbf{v}_C) = \mathbf{0}. \tag{14}$$

1. This condition is equivalent to the *force-closure* grasp condition and is also called *coordinative manipulability* in Nakamura et al. (1989) and *grasp stability* in Li et al. (1989). Note that this condition is not necessarily sufficient for generating an arbitrary resultant force $\mathbf{F}$ by a multifingered robot hand.

Substituting (13) yields

$$\mathbf{S}^T\mathbf{v}_h = \mathbf{W}_S^T\mathbf{T}\dot{\mathbf{r}}. \tag{15}$$

Differentiating (15), substituting (1) and (2), and solving, we have the general solution

$$\begin{aligned}\ddot{\mathbf{q}} = \mathbf{J}^+[&(\mathbf{S}^T)^+\{\mathbf{W}_S^T\mathbf{T}\ddot{\mathbf{r}} + (\mathbf{W}_S^T\mathbf{T})'\dot{\mathbf{r}} - \dot{\mathbf{S}}^T\mathbf{J}\dot{\mathbf{q}}\} \\ &+\{\mathbf{I}_{6k} - (\mathbf{S}^T)^+\mathbf{S}^T\}\mathbf{d}_{ah} - \dot{\mathbf{J}}\dot{\mathbf{q}}] + (\mathbf{I}_n - \mathbf{J}^+\mathbf{J})\mathbf{d}_q,\end{aligned} \tag{16}$$

where $(\cdot)'$ denotes the time derivative of $(\cdot)$. This shows the relation between the accelerations of the joints and the object. Here $\mathbf{d}_{ah}$ and $\mathbf{d}_q$ are arbitrary constant vectors and the terms $\{\mathbf{I}_{6k} - (\mathbf{S}^T)^+\mathbf{S}^T\}\mathbf{d}_{ah}$ and $(\mathbf{I}_n - \mathbf{J}^+\mathbf{J})\mathbf{d}_q$ represent the arm motions that do not affect the object motion (the former appears when some degrees of freedom of the relative motion between end effector and object remain, namely, $d = \mathrm{rank}\mathbf{S} < 6k$, whereas the latter appears when some arms have redundancy). Equation (16) gives all the possible joint accelerations that realize the object acceleration $\ddot{\mathbf{r}}$.

2.4. *Description of Object Motion Constraints*

Following Yoshikawa (1987), it is assumed that the constraints of the object motion resulting from interaction with the environment can be described by a set of hypersurfaces in the space of object position vector $\mathbf{r}$

$$p_i(\mathbf{r}) = 0, \quad i = 1, 2, \ldots, C, C \leq 6, \tag{17}$$

and that there exists a set of $(6 - C)$ scalar functions $s_j(\mathbf{r})(j = 1, 2, \ldots, (6 - C))$, and the constrained object position $\mathbf{r}_P \in \mathbf{R}^{6-C}$ is specified by

$$\mathbf{r}_P = [s_1(\mathbf{r}), s_2(\mathbf{r}), \ldots, s_{6-C}(\mathbf{r})]^T, \tag{18}$$

where $\{p_i(\mathbf{r}), i = 1, 2, \ldots, C;\ s_j(\mathbf{r}), j = 1, 2, \ldots, (6 - C)\}$ are mutually independent at any instant in time and differentiable twice with respect to $\mathbf{r}$. Differentiating (17) and (18) yields, respectively,

$$\mathbf{E}_F\dot{\mathbf{r}} = \mathbf{0}, \tag{19}$$

$$\mathbf{E}_F\ddot{\mathbf{r}} + \dot{\mathbf{E}}_F\dot{\mathbf{r}} = \mathbf{0}, \tag{20}$$

where $\mathbf{E}_F \triangleq [\mathbf{e}_{7-C} \ \mathbf{e}_{8-C} \ldots \mathbf{e}_6]^T \in \mathbf{R}^{C\times 6}$, $\mathbf{e}_{6-C+i} \triangleq \partial p_i(\mathbf{r})/\partial\mathbf{r} \in \mathbf{R}^6$, and

$$\dot{\mathbf{r}}_P = \mathbf{E}_P\dot{\mathbf{r}}, \tag{21}$$

$$\ddot{\mathbf{r}}_P = \mathbf{E}_P\ddot{\mathbf{r}} + \dot{\mathbf{E}}_P\dot{\mathbf{r}}, \tag{22}$$

where $\mathbf{E}_P \triangleq [\mathbf{e}_1 \ \mathbf{e}_2 \ldots \mathbf{e}_{6-C}]^T \in \mathbf{R}^{(6-C)\times 6}$, $\mathbf{e}_j \triangleq \partial s_j(\mathbf{r})/\partial\mathbf{r} \in \mathbf{R}^6$. Note that $\mathbf{e}_{7-C}, \mathbf{e}_{8-C}, \ldots, \mathbf{e}_6$ are vectors in the normal directions of the constraint surfaces denoting the directions of force control, while $\mathbf{e}_1, \mathbf{e}_2, \ldots, \mathbf{e}_{6-C}$

are vectors denoting the directions of position control. Figure 2 shows these vectors in the two-dimensional case with a constraint surface. By taking the present object position $\mathbf{r}$ as the origin and $\{\mathbf{e}_1, \mathbf{e}_2, \ldots, \mathbf{e}_6\}$ as bases, a constraint frame is formed. $\mathbf{E} = [\mathbf{E}_P^T\ \mathbf{E}_F^T]^T \in \mathbf{R}^{6\times 6}$ is the transformation matrix from the reference frame to the constraint frame.

This hypersurface description of the constraints of object motion will play an essential role in deriving the dynamics of the whole system and in establishing the nonlinear feedback law that linearizes and decouples the system dynamics rigorously, as seen in the following sections.

3. Equation of Motion for an Arm-Object System

The equation of motion for the arm-object system will be derived in this section. First, suppose that the joint driving force τ_C is applied to the arms at state $(\mathbf{q},\dot{\mathbf{q}})$ while holding an object under constraint (17) and that the force exerted from the end effectors on the object in directions expressed by column vectors of $\mathbf{S}$ defined in Section 2 is then $\mathbf{F}_{hS}$. Then the joint driving force that contributes to arm motion is represented by $\tau_C - \mathbf{J}^T\mathbf{S}\mathbf{F}_{hS}$ from (10) and (1). Therefore, from (3), the equation of motion of the arms holding an object is given by

$$\mathbf{M}\ddot{\mathbf{q}} + \mathbf{J}^T\mathbf{S}\mathbf{F}_{hS} = \mathbf{b}_1, \tag{23}$$

where

$$\mathbf{b}_1 \triangleq \tau_C - \mathbf{h}. \tag{24}$$

Second, let $\mathbf{f}_F \in \mathbf{R}^C$ denote the force applied from the object on the constraint surfaces in their normal directions. From (4) and (19), the same force expressed in the reference frame is given by $\mathbf{T}^{-T}\mathbf{E}_F^T\mathbf{f}_F$. Hence, from (11), the resultant force contributing to the object motion is

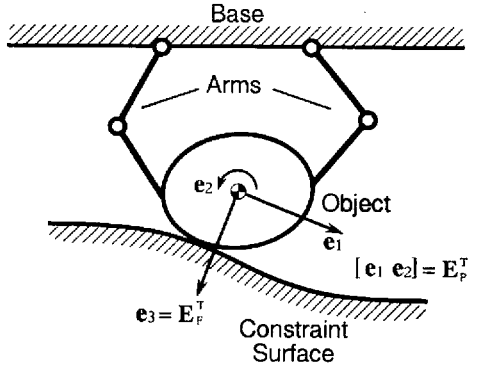

Fig. 2. Two-dimensional example of control directions of object.

given by $\mathbf{W}_S\mathbf{F}_{hS} - \mathbf{T}^{-T}\mathbf{E}_F^T\mathbf{f}_F$. Thus, from (5), the equation of motion of the object keeping contact with its environment is given by $\mathbf{I}_B\mathbf{T}\ddot{\mathbf{r}} + \mathbf{Q}_r = \mathbf{W}_S\mathbf{F}_{hS} - \mathbf{T}^{-T}\mathbf{E}_F^T\mathbf{f}_F$ or, multiplied by $\mathbf{T}^T$ left to the equation, by

$$\mathbf{T}^T\mathbf{I}_B\mathbf{T}\ddot{\mathbf{r}} - \mathbf{T}^T\mathbf{W}_S\mathbf{F}_{hS} + \mathbf{E}_F^T\mathbf{f}_F = \mathbf{b}_2, \tag{25}$$

where

$$\mathbf{b}_2 \triangleq -\mathbf{T}^T\mathbf{Q}_r. \tag{26}$$

Differentiating (15) and then using (2) and rewriting (20) yields, respectively,

$$\mathbf{S}^T\mathbf{J}\ddot{\mathbf{q}} - \mathbf{W}_S^T\mathbf{T}\ddot{\mathbf{r}} = \mathbf{b}_3, \tag{27}$$

$$\mathbf{E}_F\ddot{\mathbf{r}} = \mathbf{b}_4, \tag{28}$$

where

$$\mathbf{b}_3 \triangleq (\mathbf{W}_S^T\mathbf{T})'\dot{\mathbf{r}} - (\mathbf{S}^T\mathbf{J})'\dot{\mathbf{q}}, \tag{29}$$

$$\mathbf{b}_4 \triangleq -\dot{\mathbf{E}}_F\dot{\mathbf{r}}. \tag{30}$$

From (23), (25), (27), and (28), the equation of motion of the whole system is given by

$$\mathbf{K}\mathbf{X} = \mathbf{B}, \tag{31}$$

where $\mathbf{X} \triangleq [\ddot{\mathbf{q}}^T\ \ddot{\mathbf{r}}^T\ \mathbf{f}_{hS}^T\ \mathbf{f}_F^T]^T \in \mathbf{R}^{(n+6+d+C)}$, $\mathbf{B} \triangleq [\mathbf{b}_1^T\ \mathbf{b}_2^T\ \mathbf{b}_3^T\ \mathbf{b}_4^T]^T \in \mathbf{R}^{(n+6+d+C)}$, and

$$\mathbf{K} \triangleq \begin{bmatrix} \mathbf{M} & \mathbf{0} & \mathbf{J}^T\mathbf{S} & \mathbf{0} \\ \mathbf{0} & \mathbf{T}^T\mathbf{I}_B\mathbf{T} & -\mathbf{T}^T\mathbf{W}_S & \mathbf{E}_F^T \\ \mathbf{S}^T\mathbf{J} & -\mathbf{W}_S^T\mathbf{T} & \mathbf{0} & \mathbf{0} \\ \mathbf{0} & \mathbf{E}_F & \mathbf{0} & \mathbf{0} \end{bmatrix} \in \mathbf{R}^{(n+6+d+C)\times(n+6+d+C)}.$$

Here, $\mathbf{K}$ is a square coefficient matrix and can be shown to be nonsingular when $\mathbf{W}_S$ and $\mathbf{J}$ are of full rank (see Appendix A). Because we can calculate $\mathbf{b}_1$, $\mathbf{b}_2$, $\mathbf{b}_3$, and $\mathbf{b}_4$ from the given values of the joint driving force τ_C and the arm states $\mathbf{q}$ and $\dot{\mathbf{q}}$, by solving (31), we can find the system's behavior expressed by vector $\mathbf{X}$.

Note that the elements of variables $\ddot{\mathbf{q}}$ and $\ddot{\mathbf{r}}$ are coupled and subject to the kinematic constraints expressed by (27) and (28). As mentioned earlier, kinematic constraints (27) and (28) form an integral part of the dynamic equation of the entire system, which forms the basis for the control law for the system; this will be shown in the next section.

Forming a dynamic equation for a constrained robot system explicitly involving kinematic constraints was also suggested in McClamroch (1986). This results in derivation of a singular system of differential equations or an equivalent reduced nonsingular representation to enable the ordinary analysis of the dynamics and control of the system. However, no control law was shown, but McClamroch suggested it should be based on the proposed model.

4. Coordinated Dynamic Hybrid Controller

In this section, we present a coordinated dynamic hybrid controller consisting of linearizing and servo compensators. We assume that $\mathbf{W}_S$ has full rank and that the arms are not in singular configurations (i.e., $\mathbf{J}$ has full rank). Consider the following nonlinear state feedback law for joint driving force τ_C:

$$\tau_C = \tau_A + \tau_E, \tag{32}$$

$$\tau_A = \mathbf{M}\ddot{\mathbf{q}}_d + \mathbf{h}, \tag{33}$$

$$\begin{aligned}\ddot{\mathbf{q}}_d = \mathbf{J}^+[&(\mathbf{S}^T)^+\{\mathbf{W}_S^T\mathbf{T}\ddot{\mathbf{r}}_d + (\mathbf{W}_S^T\mathbf{T})'\dot{\mathbf{r}} - \dot{\mathbf{S}}^T\mathbf{J}\dot{\mathbf{q}}\} \\ &+ \{\mathbf{I}_{6k} - (\mathbf{S}^T)^+\mathbf{S}^T\}\mathbf{d}_{ahd} - \dot{\mathbf{J}}\dot{\mathbf{q}}] \\ &+ (\mathbf{I}_n - \mathbf{J}^+\mathbf{J})\mathbf{d}_{qd},\end{aligned} \tag{34}$$

$$\ddot{\mathbf{r}}_d = \mathbf{E}^{-1}\begin{bmatrix}\mathbf{u}_1 - \dot{\mathbf{E}}_P\dot{\mathbf{r}} \\ -\dot{\mathbf{E}}_F\dot{\mathbf{r}}\end{bmatrix}, \tag{35}$$

$$\tau_E = \mathbf{J}^T\mathbf{S}\mathbf{F}_{hSd}, \tag{36}$$

$$\begin{aligned}\mathbf{F}_{hSd} = \mathbf{W}_S^+(&\mathbf{I}_B\mathbf{T}\ddot{\mathbf{r}}_d \\ &+ \mathbf{Q}_r + \mathbf{T}^{-T}\mathbf{E}_F^T\mathbf{u}_2) + \mathbf{A}_S\mathbf{u}_3,\end{aligned} \tag{37}$$

where $\mathbf{d}_{ahd}$ and $\mathbf{d}_{qd}$ in (34) are arbitrary constant vectors that can provide arm motion that does not affect the object's motion in order to meet some given specification or criterion. Calculating $\mathbf{b}_1$, $\mathbf{b}_2$, $\mathbf{b}_3$, and $\mathbf{b}_4$ using (24), (26), (29), and (30), from (31), we obtain

$$\begin{bmatrix}\ddot{\mathbf{q}} \\ \ddot{\mathbf{r}} \\ \mathbf{f}_{hS} \\ \mathbf{f}_F\end{bmatrix} = \begin{bmatrix}\ddot{\mathbf{q}}_d \\ \ddot{\mathbf{r}}_d \\ \mathbf{f}_{hSd} \\ \mathbf{u}_2\end{bmatrix}. \tag{38}$$

From (22), (38), and (35) and from (12), (38), and (37), we can further obtain

$$\ddot{\mathbf{r}}_P = \mathbf{u}_1, \tag{39}$$

$$\mathbf{f}_F = \mathbf{u}_2, \tag{38'}$$

$$\mathbf{f}_{IS} = \mathbf{u}_3, \tag{40}$$

respectively. More detailed derivation of (38), (39), and (40) is given in Appendix B. Equations (39), (38'), and (40) mean that the system is linearized and decoupled.

Let $\ddot{\mathbf{r}}_{Pd}$ be the desired acceleration of object motion, $\mathbf{f}_{Fd}$ the desired constraint force, and $\mathbf{f}_{ISd}$ the desired internal force. If there are no modeling errors and disturbances, by taking the input vectors $\mathbf{u}_1$, $\mathbf{u}_2$, and $\mathbf{u}_3$ as $\mathbf{u}_1 = \ddot{\mathbf{r}}_{Pd}$, $\mathbf{u}_2 = \mathbf{f}_{Fd}$, and $\mathbf{u}_3 = \mathbf{f}_{ISd}$, we get $\ddot{\mathbf{r}}_P = \ddot{\mathbf{r}}_{Pd}$, $\mathbf{f}_F = \mathbf{f}_{Fd}$, and $\mathbf{f}_{IS} = \mathbf{f}_{ISd}$, and so the desired trajectories are all realized.

To cope with modeling errors and disturbances that are inevitable in real applications, we consider the following servo compensation instead of the pure feedforward law:

$$\mathbf{u}_1 = \ddot{\mathbf{r}}_{Pd} + \mathbf{K}_V(\dot{\mathbf{r}}_{Pd} - \dot{\mathbf{r}}_P) + \mathbf{K}_P(\mathbf{r}_{Pd} - \mathbf{r}_P), \tag{41}$$

$$\mathbf{u}_2 = \mathbf{f}_{Fd} + \mathbf{K}_{IF}\int_{t_0}^{t}(\mathbf{f}_{Fd} - \mathbf{f}_F)d\tau, \tag{42}$$

$$\mathbf{u}_3 = \mathbf{f}_{ISd} + \mathbf{K}_{II}\int_{t_0}^{t}(\mathbf{f}_{ISd} - \mathbf{f}_{IS})d\tau. \tag{43}$$

Then we have

$$(\ddot{\mathbf{r}}_P - \ddot{\mathbf{r}}_{Pd}) + \mathbf{K}_V(\dot{\mathbf{r}}_P - \dot{\mathbf{r}}_{Pd}) + \mathbf{K}_P(\mathbf{r}_P - \mathbf{r}_{Pd}) = \mathbf{0}, \tag{44}$$

$$(\mathbf{f}_F - \mathbf{f}_{Fd}) + \mathbf{K}_{IF}\int_{t_0}^{t}(\mathbf{f}_F - \mathbf{f}_{Fd})d\tau = \mathbf{0}, \tag{45}$$

$$(\mathbf{f}_{IS} - \mathbf{f}_{ISd}) + \mathbf{K}_{II}\int_{t_0}^{t}(\mathbf{f}_{IS} - \mathbf{f}_{ISd})d\tau = \mathbf{0}. \tag{46}$$

By choosing the feedback gain matrices $\mathbf{K}_V$, $\mathbf{K}_P$, $\mathbf{K}_{IF}$, and $\mathbf{K}_{II}$ appropriately, we can expect that the servo compensators (41), (42), and (43) will provide certain capacity for compensating for modeling errors and disturbances. Choosing feedback gain matrices as diagonal will make the closed-loop system keep the decoupled characteristics of the linearized system, while nondiagonal ones will realize coupled control purposes. A block diagram of the control system is shown in Figure 3.

Note that, letting $C = 0$ in (17), the above derived formulations can easily be adapted to the problem of controlling object motion in free space by regarding it as the case of no constraint on object motion, with $\mathbf{r}_P = \mathbf{r}$ and $\mathbf{f}_F = 0$.

5. Experiments

To examine the effectiveness of the proposed approach, three simple experiments in manipulating an object using two two-jointed robots in the horizontal plane were performed.

5.1. *Outline of the Robot System*

The two miniature robots shown in Figure 4 and made by Daikin Industries Ltd. were used for the experiments. Although each robot has three joints, only the distal two were used; these joints were called joints 1 and 2. The joints were driven by DC servo motors with a gear ratio of 1:8. The joint angles were measured using potentiometers on each joint, and the joint velocities were determined by using differential operating circuits with the potentiometer signals as the inputs. A hand-made force sensor that can measure three orthogonal translational forces and three orthogonal torques was mounted on the tip of each robot.

The model of the robot is shown in Figure 5, and the values of its parameters are given in Table 1: m_i is the mass of link i; l_i is the length of link i; l_{gi} is the length between joint i and the mass center of link i; and I_i is

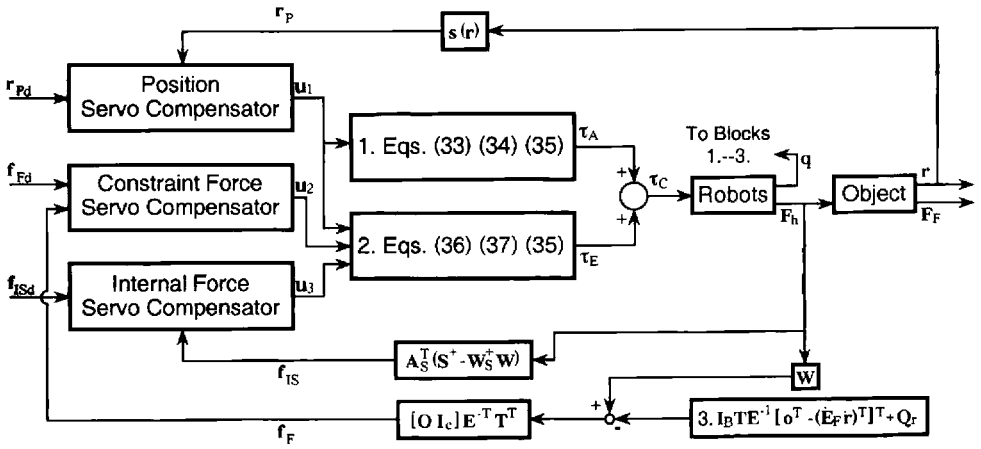

Fig. 3. Coordinated dynamic hybrid control system.

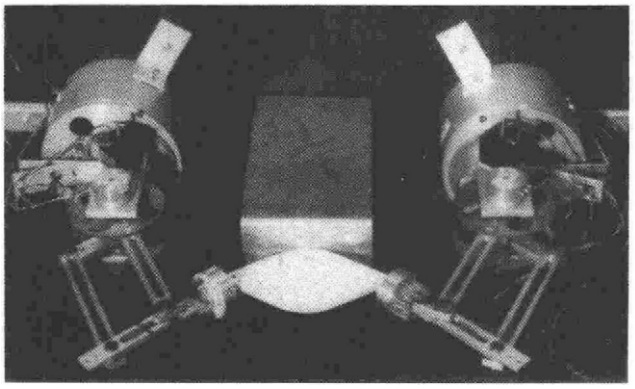

Fig. 4. Robot system.

the moment of inertia of link i about its mass center. The dynamic equation of each robot is given by

$$\tau_1 = (A + I_0 + I_2)\ddot{q}_1 + (-RC_{1-2})\ddot{q}_2 + (-RS_{1-2})\dot{q}_2^2,$$
$$\tau_2 = (-RC_{1-2})\ddot{q}_1 + (B + I_1 + I_3 + I_4)\ddot{q}_2 + (RS_{1-2})\dot{q}_1^2,$$

where τ_i is the driving torque of joint i, S_i, C_i, S_{1-2}, and C_{1-2} denote $\sin q_i$, $\cos q_i$, $\sin(q_1 - q_2)$, and $\cos(q_1 - q_2)$, respectively, and

$$A \triangleq m_0 l_{g0}^2 + m_2 l_{g2}^2 + m_3 l_0^2 + m_4 l_0^2,$$
$$B \triangleq m_1 l_{g1}^2 + m_2 l_1^2 + m_3 l_{g3}^2 + m_4 l_{g4}^2,$$
$$R \triangleq m_2 l_1 l_{g2} + m_3 l_0 l_{g3} - m_4 l_0 l_{g4}.$$

As shown in Figure 2, the robot system was linearized by linearization compensators represented by (32)–(37), and servo compensators, represented by (41)–(43), were added to the linearized system. This control algorithm was implemented using a 32-bit personal computer with a floating point processing unit (FPU) and programmed using C and assembly languages. The resulting sampling rate was 2 ms (i.e., 500 Hz).

5.2. *Task Description*

The first task was a constrained motion control—that is, to grasp an object with mass of 0.03 kg and moment of inertia about its mass center of 14.4×10^{-5} kgm^2 and to move it along the constraint surface following a desired trajectory profile while keeping the contact force to a desired value. A plane surface parallel to the x axis of Σ_O was selected as the constraint surface. The object had two holes, and each arm had a pin at its tip. The arms could pull or push the object after inserting their pins into the holes. For this system, the constrained object position $\mathbf{r}_P$ was specified by $\mathbf{r}_P = [x\ \phi]^T$, where x is the translational position along the surface and ϕ is the orientation with respect to the surface. The constraint force was normal to the constraint plane, specified by f_F (Fig. 6). The internal force was the average of two opposite pushing forces applied by the two arms, lying

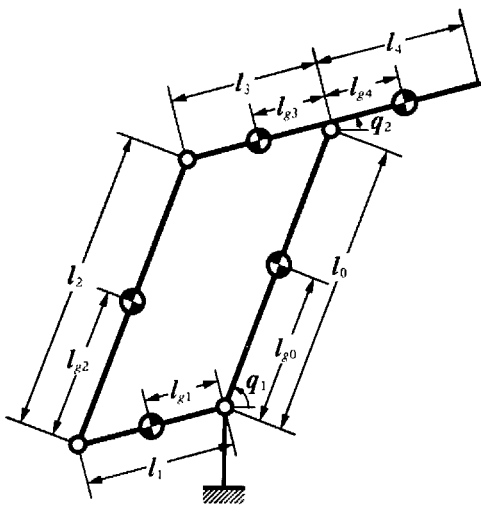

Fig. 5. Model of robot.

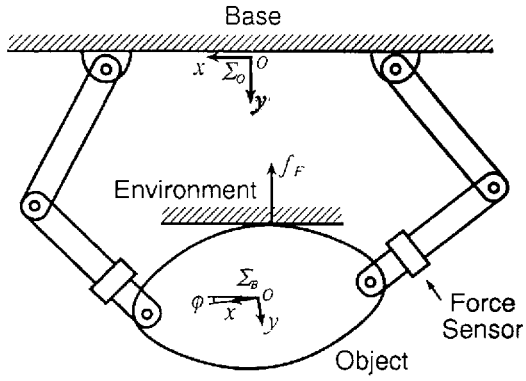

Fig. 6. Diagram of experimental setup.

along the line passing through the two pins of the arms and specified by f_{IS}.

The second task was to move the object without constraint on its motion and with $\mathbf{r}_P$ specified by $\mathbf{r}_P = \mathbf{r} = [x\ y\ \phi]^T$, where x and y are the translational position with respect to Σ_O, and ϕ is the orientation.

The third task included a series of control phases consisting of free motion, contact with a rigid surface, constrained motion, departure from the surface, and return to free motion, assuming those tasks during which the manipulated object encounters the surrounding environment.

5.3. *Results*

The desired translational position trajectory in the x direction was a move through 0.05 m during 0.8 s, with the phases of acceleration, constant velocity, and deceleration; in the y direction for second and third tasks, the trajectory was a forth-and-back motion through 0.025 m for the same duration and with the same motion patterns. The trajectories during acceleration and deceleration were given by fourth-order polynomials of time. The desired orientational position trajectory was a constant (i.e., the initial orientation was maintained throughout the task). The surface used in the experiments was an aluminum plane, which the object impacted at a velocity of 0.068 m/s in its normal direction during the third task.

Table 1. Parameter Values of Robot

Link	m_i ($\times 10^{-3}$kg)	l_i ($\times 10^{-3}$m)	l_{gi} ($\times 10^{-3}$m)	I_i ($\times 10^{-5}$kgm^2)
0	29.0	128.0	68.0	16.40
1	19.5	50.0	30.0	6.24
2	28.5	128.0	64.0	8.96
3	23.9	50.0	25.0	0.75
4	30.0	63.0	40.0	5.00

The desired constraint force for the first and third tasks and the internal force trajectories were assigned as given in Table 2.

In the third experiment, motion control was switched to force control in the direction of constraint when the object came into contact with the constraint surface and the contact force reached a certain value.

The parameters of the servo compensators were as follows:

$$\mathbf{K}_V = \text{diag}[65, 50, 55],$$
$$\mathbf{K}_P = \text{diag}[13000, 13000, 15000],$$
$$\mathbf{K}_{IF} = [100], \quad \mathbf{K}_{II} = [70].$$

These were selected by trial-and-error to ensure the closed-loop systems (44), (45), and (46) were stable and had good transient and steady response to the desired trajectories with rapid convergence and small steady error in each of the three experiments.

The desired trajectories and the results of the three experiments are shown in Figures 7–9. From the figures, it can be seen that the translational and orientational positions, constraint force, and internal force were all controlled well and that the desired constraint force and internal force were also followed well. The transition from free to constrained motion was fairly smooth.

In those experiments that included constrained motion, no explicit friction model was included in the system dynamics, although some friction force did certainly exist (e.g., such as that between the moving object and the constraint plane along the direction of motion). The experimental results showed that the unmodeled friction force, which was assumed could be regarded as disturbance to the system, was servo-compensated effectively, as expected.

6. Conclusions

A coordinated dynamic hybrid control method for multiple robotic mechanisms handling a single object whose motion may be constrained by the environment has been discussed. The method takes manipulator dynamics and object dynamics into consideration and can be used to control the motion of the object as well as the con-

Table 2. Desired Trajectories of Constraint and Internal Force

Time(s)	Constraint force(N)	Internal force(N)
$0.0 \sim 0.27$	0.50	0.8
$0.27 \sim 0.53$	0.75	1.0
$0.53 \sim 0.8$	0.50	0.8

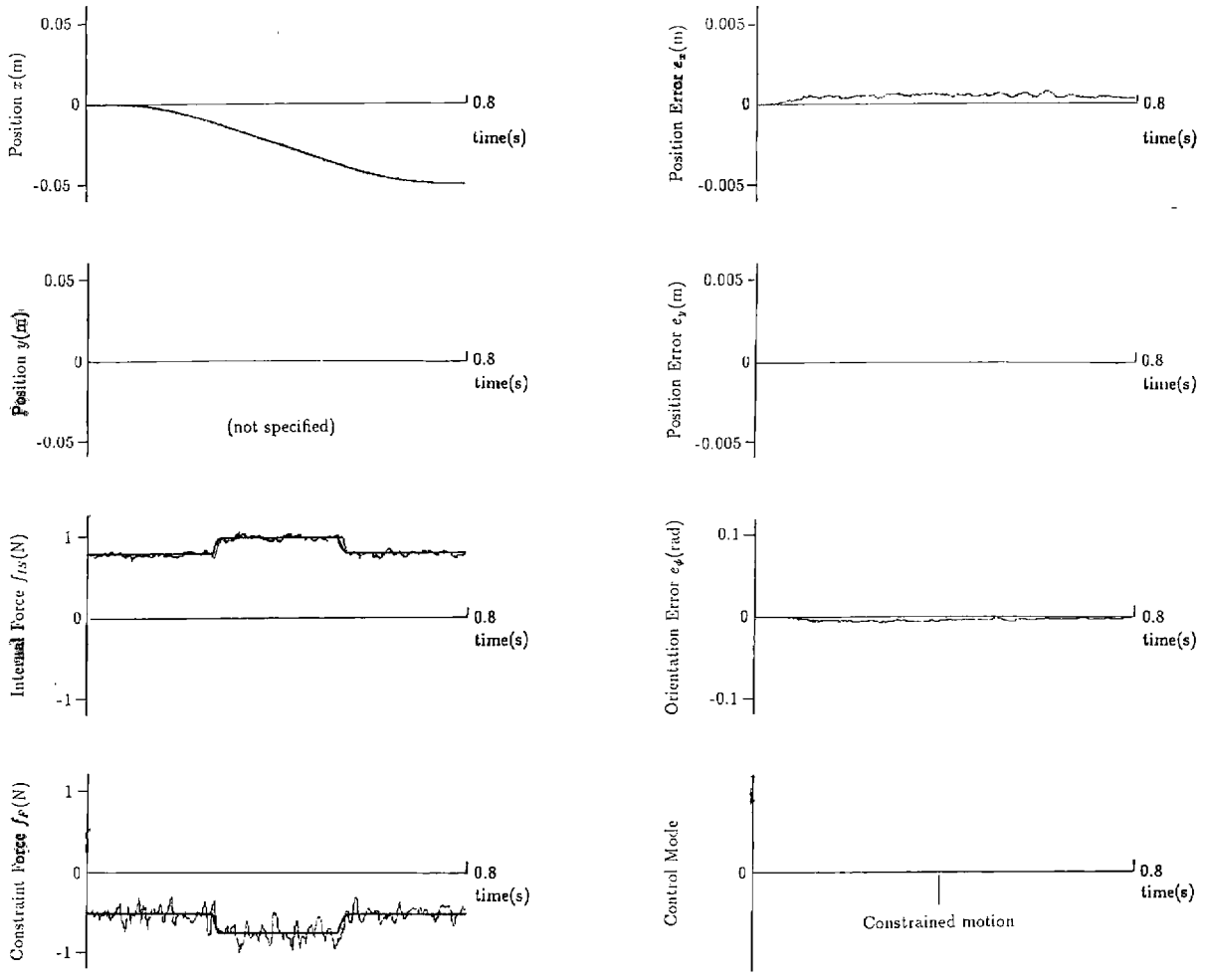

Fig. 7. Experimental results 1. —, Constrained motion.

straint force when the object motion constraint occurs and the internal force. We have achieved the following results:

1. The dynamic equation of the entire arm-object system has been derived. This explicitly involved the unified formulation of the force and kinematic constraint on various grasp types and the hypersurface description of object motion constraint.

2. A nonlinear state feedback law for the joint driving force has been given that linearizes and decouples the system with respect to the object motion, constraint force, and internal force. The basic structure of the dynamic hybrid control system with a servo compensator has also been presented. Controlling free object motion can be treated as a special case within the same formulation.

3. The effectiveness of the approach was verified by several experiments.

These results are useful for fine manipulation tasks, such as assembly using multiple robotic mechanisms, where individual specification of the object motion, the interaction force between the object and its environment, and the grasping force of the object is necessary.

Appendix A: Nonsingularity of Matrix K

The nonsingularity of $\mathbf{K}$ under the assumption that $\mathbf{W}_S$ and $\mathbf{J}$ are of full rank can be proved as follows. Adapting elementary transformation to $\mathbf{K}$ in terms of its blocks yields

$$\mathbf{K} \sim \begin{bmatrix} \mathbf{M} & \mathbf{0} & \mathbf{J}^T\mathbf{S} & \mathbf{0} \\ \mathbf{0} & \mathbf{T}^T\mathbf{I}_B\mathbf{T} & \mathbf{K}_{23} & \mathbf{E}_F^T \\ \mathbf{0} & \mathbf{0} & \mathbf{K}_{33} & \mathbf{0} \\ \mathbf{0} & \mathbf{0} & \mathbf{0} & \mathbf{E}_F\mathbf{T}^{-1}\mathbf{I}_B^{-1}\mathbf{T}^{-T}\mathbf{E}_F^T \end{bmatrix}, \quad \text{(A1)}$$

where

$$\mathbf{K}_{23} = \mathbf{E}_F^T(\mathbf{E}_F\mathbf{T}^{-1}\mathbf{I}_B^{-1}\mathbf{T}^{-T}\mathbf{E}_F^T)^{-1}\mathbf{E}_F\mathbf{T}^{-1}\mathbf{I}_B^{-1}\mathbf{W}_S - \mathbf{T}^T\mathbf{W}_S, \quad \text{(A2)}$$

$$\mathbf{K}_{33} = \mathbf{S}^T\mathbf{J}\mathbf{M}^{-1}\mathbf{J}^T\mathbf{S} + \mathbf{W}_S^T\mathbf{I}_B^{-1}\mathbf{W}_S - \mathbf{W}_S^T\mathbf{I}_B^{-1}\mathbf{T}^{-T}\mathbf{E}_F^T \times (\mathbf{E}_F\mathbf{T}^{-1}\mathbf{I}_B^{-1}\mathbf{T}^{-T}\mathbf{E}_F^T)^{-1}\mathbf{E}_F\mathbf{T}^{-1}\mathbf{I}_B^{-1}\mathbf{W}_S. \quad \text{(A3)}$$

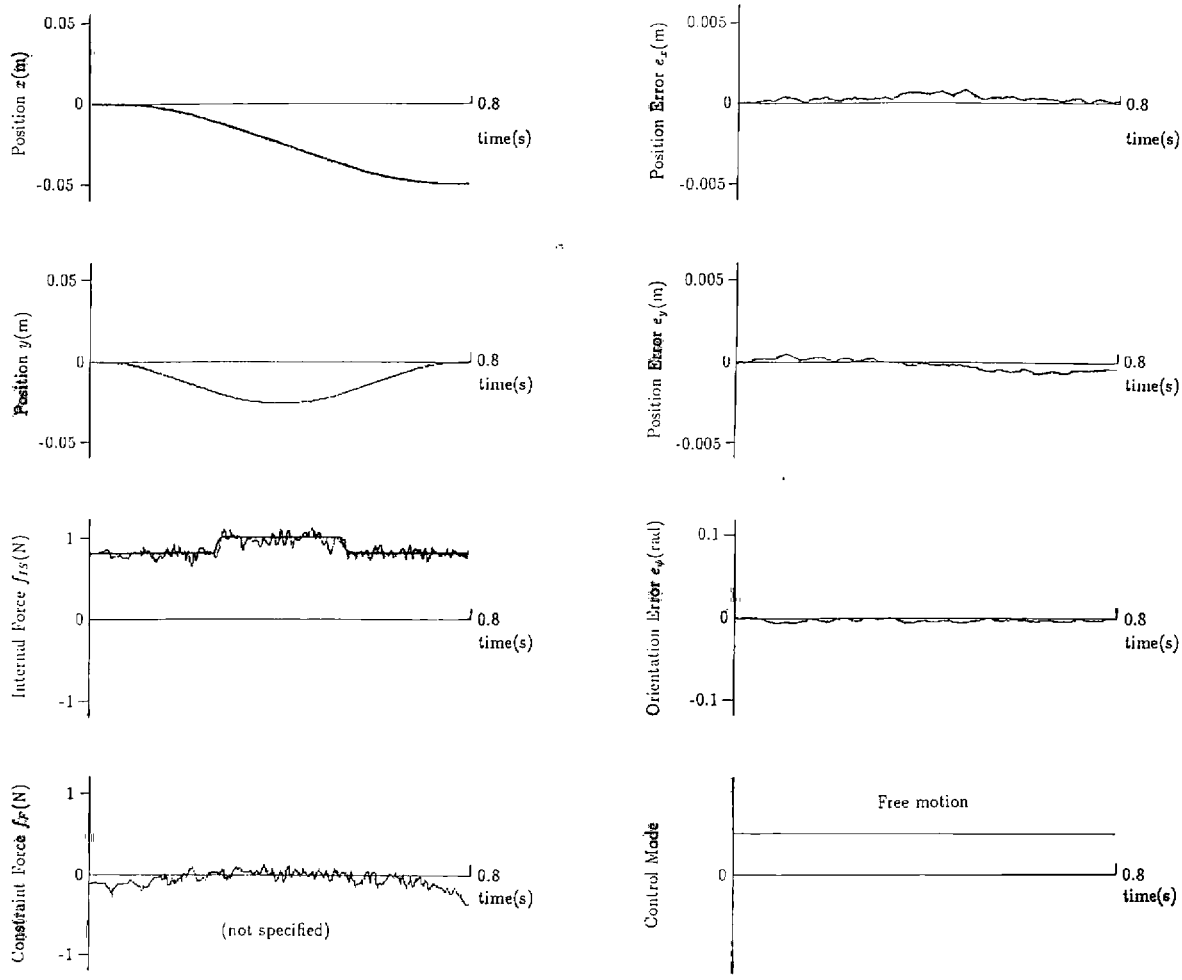

Fig. 8. Experimental results 2. —, Free motion.

Because $\mathbf{I}_B$ is a positive definite symmetric matrix, there exists a nonsingular matrix $\hat{\mathbf{I}}_B$ such that $\mathbf{I}_B = \hat{\mathbf{I}}_B^T\hat{\mathbf{I}}_B$. Then,

$$\begin{aligned}\mathbf{K}_{33} &= \mathbf{S}^T\mathbf{J}\mathbf{M}^{-1}\mathbf{J}^T\mathbf{S} \\ &\quad + \mathbf{W}_S^T\hat{\mathbf{I}}_B^{-1}\Big\{\mathbf{I}_6 - \hat{\mathbf{I}}_B^{-T}\mathbf{T}^{-T}\mathbf{E}_F^T(\mathbf{E}_F\mathbf{T}^{-1}\hat{\mathbf{I}}_B^{-1}\hat{\mathbf{I}}_B^{-T}\mathbf{T}^{-T}\mathbf{E}_F^T)^{-1} \\ &\qquad \times \mathbf{E}_F\mathbf{T}^{-1}\hat{\mathbf{I}}_B^{-1}\Big\}\hat{\mathbf{I}}_B^{-T}\mathbf{W}_S \\ &\triangleq \mathbf{S}^T\mathbf{J}\mathbf{M}^{-1}\mathbf{J}^T\mathbf{S}\mathbf{W}_S^T\hat{\mathbf{I}}_B^{-1}\big\{\mathbf{I}_6 - \hat{\mathbf{A}}^T(\hat{\mathbf{A}}\hat{\mathbf{A}}^T)^{-1}\hat{\mathbf{A}}\big\}\hat{\mathbf{I}}_B^{-T}\mathbf{W}_S, \qquad \text{(A4)}\end{aligned}$$

where

$$\hat{\mathbf{A}} \triangleq \mathbf{E}_F\mathbf{T}^{-1}\hat{\mathbf{I}}_B^{-1}. \qquad \text{(A5)}$$

The first term on the right side of (A4) is positive definite as a result of the assumption that $\mathbf{W}_S$ and $\mathbf{J}$ are of full rank. Noting that $\hat{\mathbf{A}}^T(\hat{\mathbf{A}}\hat{\mathbf{A}}^T)^{-1}$ represents the pseudoinverse of $\hat{\mathbf{A}}$, $\hat{\mathbf{A}}^+$ and that $\mathbf{I}_6 - \hat{\mathbf{A}}^+\hat{\mathbf{A}} \geq 0$ holds, it can be seen that the second term of (A4) is nonnegative definite. Therefore, $\mathbf{K}_{33} > 0$ holds. Hence, all the diagonal blocks of the right side of (A1) are nonsingular, implying that $\mathbf{K}$ is nonsingular.

Appendix B: Derivation of Eqs. (38), (39), and (40)

Substituting (32), (33), and (36) to (24) yields

$$\mathbf{b}_1 = \mathbf{M}\ddot{\mathbf{q}}_d + \mathbf{J}^T\mathbf{S}\mathbf{F}_{hSd}, \qquad \text{(B1)}$$

Noting that $\mathbf{W}_S\mathbf{A}_S = \mathbf{0}$, from (37),

$$\mathbf{T}^T\mathbf{W}_S\mathbf{F}_{hSd} = \mathbf{T}^T\mathbf{I}_B\mathbf{T}\ddot{\mathbf{r}}_d + \mathbf{T}^T\mathbf{Q}_r + \mathbf{E}_F^T\mathbf{u}_2, \qquad \text{(B2)}$$

and from (26) and (B2),

$$\mathbf{b}_2 = \mathbf{T}^T\mathbf{I}_B\mathbf{T}\ddot{\mathbf{r}}_d - \mathbf{T}^T\mathbf{W}_S\mathbf{F}_{hSd} + \mathbf{E}_F^T\mathbf{u}_2. \qquad \text{(B3)}$$

Noting that $\mathbf{J}\mathbf{J}^+ = \mathbf{I}_n$, $\mathbf{J}(\mathbf{I}_n - \mathbf{J}^+\mathbf{J}) = \mathbf{0}$, $\mathbf{S}^T(\mathbf{S}^T)^+ = \mathbf{I}_d$, and $\mathbf{S}^T\{\mathbf{I}_{6k} - (\mathbf{S}^T)^+\mathbf{S}^T\} = \mathbf{0}$ hold, and using (34), we have

$$\mathbf{S}^T\mathbf{J}\ddot{\mathbf{q}}_d = \mathbf{W}_S^T\mathbf{T}\ddot{\mathbf{r}}_d + (\mathbf{W}_S^T\mathbf{T})'\dot{\mathbf{r}} - (\mathbf{S}^T\mathbf{J})'\dot{\mathbf{q}}. \qquad \text{(B4)}$$

From (29) and (B4),

$$\mathbf{b}_3 = \mathbf{S}^T\mathbf{J}\ddot{\mathbf{q}}_d - \mathbf{W}_S^T\mathbf{T}\ddot{\mathbf{r}}_d. \qquad \text{(B5)}$$

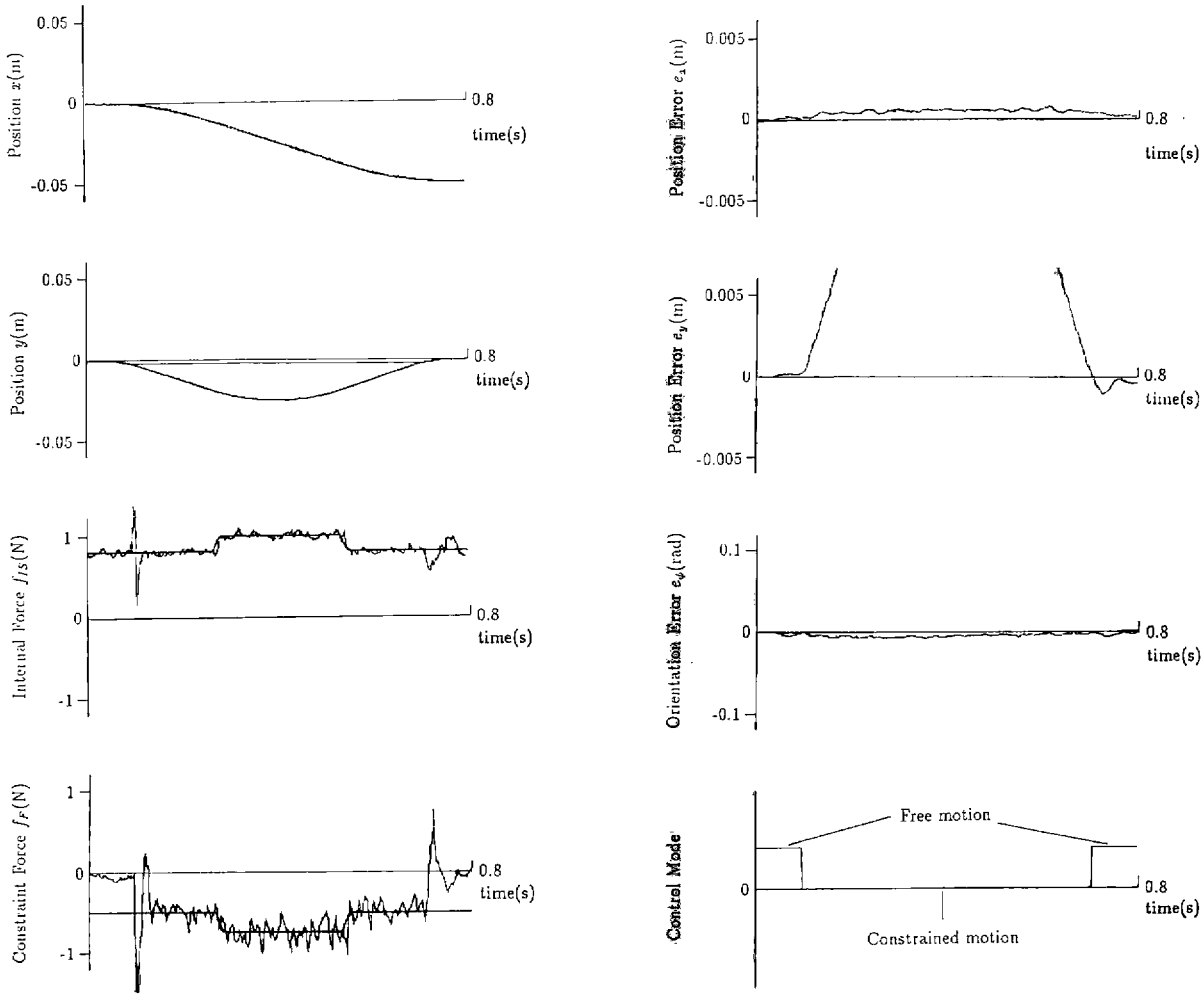

Fig. 9. Experimental results 3. —, Free to/from constrained motion.

From (35),

$$\mathbf{E}\ddot{\mathbf{r}}_d = \begin{bmatrix} \mathbf{u}_1 - \dot{\mathbf{E}}_P\dot{\mathbf{r}} \\ -\dot{\mathbf{E}}_F\dot{\mathbf{r}} \end{bmatrix}, \tag{B6}$$

or

$$\mathbf{E}_P\ddot{\mathbf{r}}_d = \mathbf{u}_1 - \dot{\mathbf{E}}_P\dot{\mathbf{r}}, \tag{B7}$$

$$\mathbf{E}_F\ddot{\mathbf{r}}_d = -\dot{\mathbf{E}}_F\dot{\mathbf{r}}, \tag{B8}$$

and from (30) and (B8),

$$\mathbf{b}_4 = \mathbf{E}_F\ddot{\mathbf{r}}_d. \tag{B9}$$

Putting (B1), (B3), (B5), and (B9) together yields

$$\mathbf{B} = \begin{bmatrix} \mathbf{M} & \mathbf{0} & \mathbf{J}^T\mathbf{S} & \mathbf{0} \\ \mathbf{0} & \mathbf{T}^T\mathbf{I}_B\mathbf{T} & -\mathbf{T}^T\mathbf{W}_S & \mathbf{E}_F^T \\ \mathbf{S}^T\mathbf{J} & -\mathbf{W}_S^T\mathbf{T} & \mathbf{0} & \mathbf{0} \\ \mathbf{0} & \mathbf{E}_F & \mathbf{0} & \mathbf{0} \end{bmatrix} \begin{bmatrix} \ddot{\mathbf{q}}_d \\ \ddot{\mathbf{r}}_d \\ \mathbf{f}_{hSd} \\ \mathbf{u}_2 \end{bmatrix}$$
$$= \mathbf{K}[\ddot{\mathbf{q}}_d^T \ \ddot{\mathbf{r}}_d^T \ \mathbf{f}_{hSd}^T \ \mathbf{u}_2^T]^T, \tag{B10}$$

which gives the right side of (31). Because $\mathbf{K} \in \mathbf{R}^{(n+6+d+C)\times(n+6+d+C)}$ is nonsingular under the assumption that $\mathbf{W}_S$ and $\mathbf{J}$ have full rank (see Appendix A), from (31) and (B10),

$$\begin{bmatrix} \ddot{\mathbf{q}} \\ \ddot{\mathbf{r}} \\ \mathbf{f}_{hS} \\ \mathbf{f}_F \end{bmatrix} = \begin{bmatrix} \ddot{\mathbf{q}}_d \\ \ddot{\mathbf{r}}_d \\ \mathbf{f}_{hSd} \\ \mathbf{u}_2 \end{bmatrix}. \tag{B11}$$

Hence, (38) is obtained. From (22), (B11), and (B7),

$$\begin{aligned} \ddot{\mathbf{r}}_P &= \mathbf{E}_P\ddot{\mathbf{r}} + \dot{\mathbf{E}}_P\dot{\mathbf{r}} \\ &= \mathbf{E}_P\ddot{\mathbf{r}}_d + \dot{\mathbf{E}}_P\dot{\mathbf{r}} \\ &= \mathbf{u}_1. \end{aligned} \tag{B12}$$

Hence, (39) is obtained. From (12) and (11),

$$\begin{aligned} \mathbf{A}_S\mathbf{f}_{IS} &= \mathbf{F}_{hS} - \mathbf{W}_S^+\mathbf{F} \\ &= \mathbf{F}_{hS} - \mathbf{W}_S^+\mathbf{W}_S\mathbf{F}_{hS} \\ &= (\mathbf{I}_d - \mathbf{W}_S^+\mathbf{W}_S)\mathbf{F}_{hS}. \end{aligned} \tag{B13}$$

Noting the orthogonality of $\mathbf{A}_S$ and that $(\mathbf{I}_d - \mathbf{W}_S^+\mathbf{W}_S)\mathbf{W}_S^+ = \mathbf{0}$, from (B13), (B11), and (37), we have

$$\begin{aligned}\mathbf{f}_{IS} &= \mathbf{A}_S^T(\mathbf{I}_d - \mathbf{W}_S^+\mathbf{W}_S)\mathbf{F}_{hS} \\ &= \mathbf{A}_S^T(\mathbf{I}_d - \mathbf{W}_S^+\mathbf{W}_S)\mathbf{F}_{hSd} \\ &= \mathbf{A}_S^T\mathbf{A}_S\mathbf{u}_3 \\ &= \mathbf{u}_3. \end{aligned} \tag{B14}$$

Hence, (40) is obtained.

References

Alberts, T. E., and Soloway, D. I. 1988. Force control of a multiarm robot system. *Proc. IEEE Int. Conf. on Robotics and Automation*, pp. 1490–1496.

Arimoto, S., Miyazaki, F., and Kawamura, S. 1987. Cooperative motion control of multiple robot arms or fingers. *Proc. IEEE Int. Conf. on Robotics and Automation*, pp. 1407–1412.

Cole, A. B. A., Hauser, J. E., and Sastry, S. S. 1989. Kinematics and control of multifingered hands with rolling contact. *IEEE Trans. Auto. Control* 34(4):398–404.

Cutkosky, M. R., and Kao, I. 1989. Computing and controlling the compliance of a robotic hand. *IEEE Trans. on Robotics and Automation* 5(2):151–165.

Hayati, S. 1986. Hybrid position/force control of multiarm cooperating robots. *Proc. IEEE Int. Conf. on Robotics and Automation*, pp. 82–89.

Khatib, O. 1987. Object manipulation in a multi-effector robot system. *Preprints 4th Int. Symp. Robotics Res.*, pp. 131–138.

Kumar, V. R., and Waldron, K. J. 1988. Force distribution in closed kinematic chains. *IEEE J. Robot. Automation* 4(6):657–664.

Li, Z. X., Hsu, P., and Sastry, S. 1989. Grasping and coordinated manipulation by a multifingered robot hand. *Int. J. Robotics Res.* 8(4):33–50.

Luh, J. Y. S., and Zheng, Y. F. 1987. Constrained relations between two coordinated industrial robots for motion control. *Int. J. Robotics Res.* 6(3):60–70.

McClamroch, N. H. 1986. Singular system of differential equations as dynamic models for constrained robot systems. *Proc. IEEE Int. Conf. on Robotics and Automation*, pp. 21–28.

Nakamura, Y., Nagai, K., and Yoshikawa, T. 1989. Dynamics and stability in coordination of multiple robotic mechanisms. *Int. J. Robotics Res.* 8(2):44–61.

Nakano, E., Ozaki, S., Ishida, T., and Kato, I. 1974. Cooperational control of the anthropomorphous manipulator 'MELARM'. *Proc. 4th Int. Symp. on Industrial Robots*, pp. 251–260, Tokyo.

Raibert, M. H., and Craig, J. J. 1981. Hybrid position/force control of manipulators. *Trans. ASME J. Dyn. Sys. Measurement Contr.* 102:126–133.

Uchiyama, M., and Dauchez, P. 1988. A symmetric hybrid position/force control scheme for the coordination of two robots. *Proc. IEEE Int. Conf. on Robotics and Automation*, pp. 350–356.

Yoshikawa, T. 1987. Dynamic hybrid position/force control of robot manipulators—description of hand constraints and calculation of joint driving force. *IEEE J. Robotics and Automation* RA-3(5):386–392.

Yoshikawa, T., and Nagai, K. 1987. Manipulating and grasping forces in manipulation by multifingered hands. *Proc. IEEE Int. Conf. on Robotics and Automation*, pp. 1998–2004.

Yoshikawa, T., Sugie, T., and Tanaka, M. 1988. Dynamic hybrid position/force control of robot manipulators—controller design and experiment. *IEEE J. Robot. Automation* RA-4(6):699–705.

Zheng, Y. F., and Luh, J. Y. S. 1989. Optimal load distribution for two industrial robots handling a single object. *Trans. ASME J. Dyn. Sys. Measurement Contr.* 111:232–237.